Improved Classification of VHR Images of Urban Areas Using Directional Morphological Profiles

Rik Bellens, *Student Member, IEEE*, Sidharta Gautama, *Member, IEEE*, Leyden Martinez-Fonte, *Member, IEEE*, Wilfried Philips, *Member, IEEE*, Jonathan Cheung-Wai Chan, and Frank Canters

***Abstract*—Meter to submeter resolution satellite images have generated new interests in extracting man-made structures in the urban area. However, classification accuracies for such purposes are far from satisfactory. Spectral characteristics of urban land cover classes are so similar that they cannot be separated using only spectral information. As a result, there is an increased interest in incorporating geometrical information. One possible approach is the use of morphological profiles (MPs). In this paper, we introduce two improvements on the use of MPs. Current approaches use disk-shaped structuring elements (SEs) to derive an MP. This profile contains information about the minimum dimension of objects. In this paper, we extend this approach by using linear SEs. This results in a profile containing information about the maximum object dimension. We show that the addition of the line-based MP gives a substantial improvement of the classification result. A second improvement is achieved by using "partial morphological reconstruction" instead of the normal morphological reconstruction. Morphological reconstruction is commonly used to better preserve the shape of objects. However, we show that this leads to "over-reconstruction" in typical remote sensing images and a decreased classification performance. With "partial reconstruction," we are able to overcome this problem and still preserve the shape of objects.**

***Index Terms*—Classification, high-resolution imagery, mathematical morphology, urban areas.**

I. Introduction

RECENT advances in Earth observation technology have led to an increased availability of data products at very high spatial resolutions. These may open up new areas in the application of satellite imagery. Land-use mapping in complex settings such as urban and suburban environments is one of the domains for which the new very high resolution (VHR) data will offer new possibilities. Of particular interest herein is the detection and identification of a variety of man-made structures such as roads and buildings. The difficulty of using VHR imagery such as IKONOS and QuickBird is that the classification accuracy for such purposes is far from satisfactory [1]. Spectral characteristics of urban land cover classes such as road surfaces, parking lots, and open areas are so similar that they cannot be separated using only spectral information. As a result, there is an increased interest in incorporating geometrical information in image classification.

Automated land-cover classification can be accomplished using either pixel-based or object-based approaches [2]–[4]. In [5], both approaches are combined. Pixel-based methods classify each pixel individually, whereas object-based methods first group together pixels in a meaningful way by image segmentation. The object-based approach provides a straightforward method to incorporate geometrical information. Different shape characteristics of objects can easily be calculated on the segments. However, the segmentation process is a very difficult task. Good parameters for the process highly depend on the image data and the classification task [4]. In pixel-based approaches, it is less straightforward to incorporate geometrical information. Consequently, most pixel-based approaches only rely on spectral and possibly textural information. However, recently, some attempts were made to derive per-pixel shape information. In [6], a length–width extraction algorithm is proposed. In [7], a pixel shape index is introduced, which measures the gray similarity distance in every direction. These methods are extended in [8] to a structural feature set.

Another possibility to incorporate geometrical information is the use of mathematical morphology [9]–[11]. Image features defined by their morphological characteristics are reportedly useful to improve accuracies in urban classifications using VHR data. In [12] and [13], a multiscale approach is used. Morphological profiles (MPs) are generated from a panchromatic image. An MP is a composition of morphological openings and closings with increasing size of the structuring element (SE). Each opening and closing results in a transformation of the original image in which objects smaller than the SE are deleted. As such, the MP carries information about the size and the shape of objects in the image. In [14], an extended MP is proposed for hyperspectral images.

In the current literature [12], [13], the MP is based on openings and closings with disk-shaped SEs. This results in an MP carrying information about the minimum dimension of objects. However, to distinguish between typical buildings (rectangles) and roads (linear shaped), one also needs information about the maximum dimension. Therefore, we introduce the use of an MP based on linear SEs or a directional MP. Using both a disk-based and a directional MP improves the classification result substantially. Directional morphological openings and closings

Manuscript received October 1, 2007; revised January 14, 2008. Current version published October 1, 2008. This work was supported in part by the Belgian Science Policy Office under the framework of the STEREO programme—Project SR/00/050 and in part by a scholarship of the "Institute for the Promotion of Innovation through Science and Technology in Flanders" (IWT-Vlaanderen).

R. Bellens, S. Gautama, L. Martinez-Fonte, and W. Philips are with the Department for Telecommunications and Information Processing, Ghent University, 9000 Ghent, Belgium (e-mail: rik.bellens@telin.ugent.be).

J. C.-W. Chan and F. Canters are with the Cartography and GIS Research Unit, Department of Geography, Vrije Universiteit Brussel, 1050 Brussels, Belgium.

Digital Object Identifier 10.1109/TGRS.2008.2000628

have been successfully used for road detection in [15] and [16]. However, these papers only use a single scale.

Classical morphological openings and closings degrade the object boundaries. Consequently, a classification based on MPs will show problems near borders of objects. To overcome this problem, a process called reconstruction [9] is generally used. Informally, this process aims at reconstructing the original shape of objects of which at least one pixel is not deleted in the opening or closing. While reconstruction has become a standard practice (see, e.g., [12] and [13]), we show in this paper that reconstruction leads to some unexpected and undesirable results for remote sensing images, and it is often better not to use it. The problem could be described as "over-reconstruction," meaning that objects we would expect to have disappeared at a certain scale remain present when using reconstruction. We will also present a new method called "partial reconstruction" based on geodesic transforms [17]. This method solves the problem of over-reconstruction while preserving the shape of objects as much as possible.

This paper is organized as follows. Section II explains the basic operations in mathematical morphology and introduces the use of MPs for describing geometrical information in VHR satellite images. Section III describes the reconstruction process as well as the problem of over-reconstruction. A solution for this problem, "partial reconstruction," is proposed in Section IV. Experimental classification results are given in Section V, and the conclusions are in Section VI.

II. Mathematical Morphology

Mathematical morphology [9], [11] is a popular tool in image processing and can be used in very diverse tasks such as feature detection, image segmentation, image denoising, image sharpening, and many more. Successful applications of mathematical morphology in remote sensing image processing can be found in [10]. In this section, we will give a short introduction to the morphological operations which are important for the remainder of this paper (for a more formal and detailed description of mathematical morphology, we refer to [9] and [11]).

Many morphological operators exist. One of them, the *opening*, is of particular importance for this paper. In a binary image, where ones are foreground pixels and zeros are background pixels, an opening erases all objects in which a certain SE does not fit. This SE can have an arbitrary size and shape. Typical shapes are disks and lines. In gray-scale images, the behavior of an opening is similar, but now, the gray-scale value of a pixel is interpreted as the fuzzy membership value of that pixel belonging to the foreground (high gray-scale values) or to the background (low gray-scale values). An opening thus results in a new image where small bright objects (compared to their surroundings) are deleted. This means that they get assigned the gray-scale value of their surroundings. Dark objects are left unchanged. The dual operation of the opening is the closing. This operator reverses the interpretation of gray-scale values and thus removes small dark objects and leaves bright objects unchanged.

Note that we use the term *object* as an informal and vague term to clarify to the reader the behavior of the different operators on remote sensing images. In reality, however, openings and closings are local operators which act on pixels and their neighborhood. There is no explicit notion of objects. As a result of this, an opening (and, similarly, a closing) not only removes certain objects but also deforms objects. Therefore, the result of an opening or closing for a certain pixel also depends on the location of that pixel in the object. As a good classification result would assign each pixel of an object to the same class, this behavior should be avoided. Solutions for this problem will be discussed in Sections III and IV.

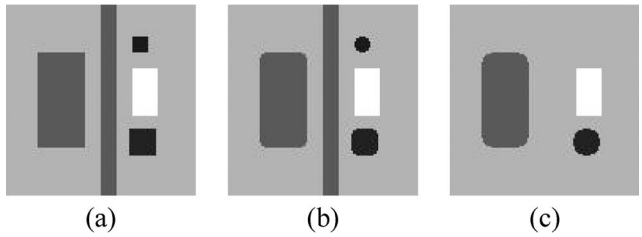

Fig. 1. (a) Image and its closings with disk-shaped SEs of sizes (b) $R = 3$ and (c) $R = 6$. Objects with a width smaller than $2 \cdot R$ are deleted from the image. As a side effect, borders of objects are smoothed.

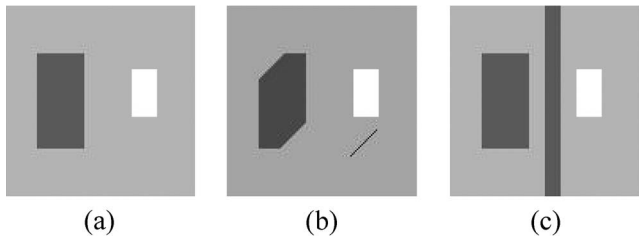

Fig. 2. Three closings with linear SEs of length L and different orientations. Dark objects with small dimensions in all directions are removed in every closing. Dark objects with a large dimension in at least one direction remain visible in some closings. (a) $L = 25$, $\theta = 0$. (b) $L = 25$, $\theta = \pi/4$. (c) $L = 25$, $\theta = \pi/2$.

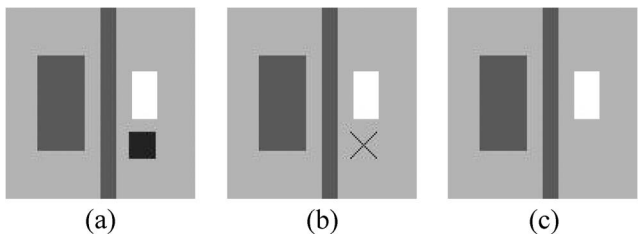

Fig. 3. Minimum of closings with linear SEs for three different lengths. Objects are filtered out if their maximum dimension is smaller than L. Rectangular objects with length smaller than L and diagonal size larger than L are partly removed. (a) $L = 15$. (b) $L = 25$. (c) $L = 35$.

A. Disk-Shaped SE

As mentioned, different shapes can be chosen for the SE. A very common shape is a disk with a radius R. Fig. 1 shows an image and two closings with disk-shaped SEs of different sizes. Objects with a width smaller than $2 \cdot R$ are deleted from the image. Closings and openings with disk-shaped SEs thus act on the minimum dimension of objects. Aside from deleting certain objects, the objects are also deformed. With disk-shaped SEs, the corners of rectangular objects are rounded. This rounding is small for small SEs and increases with its size. The distance

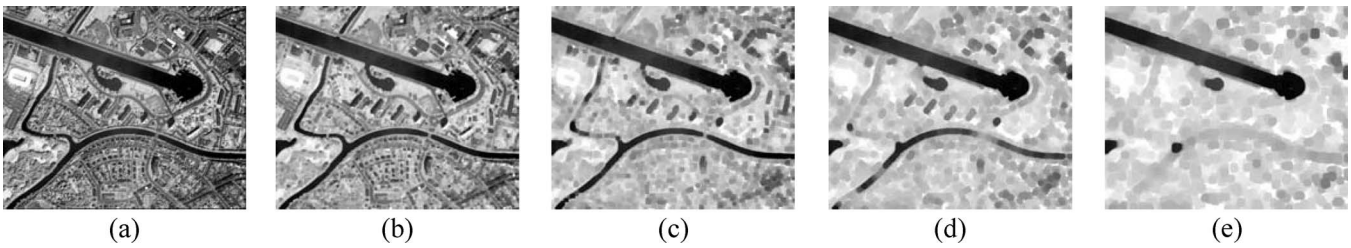

Fig. 4. Closings with disk-shaped SEs of increasing size. As the size increases, more and more objects disappear depending on their minimum dimension. The blobby effect is caused by the smoothing of object boundaries. (a) Original. (b) $R = 5$. (c) $R = 10$. (d) $R = 15$. (e) $R = 20$.

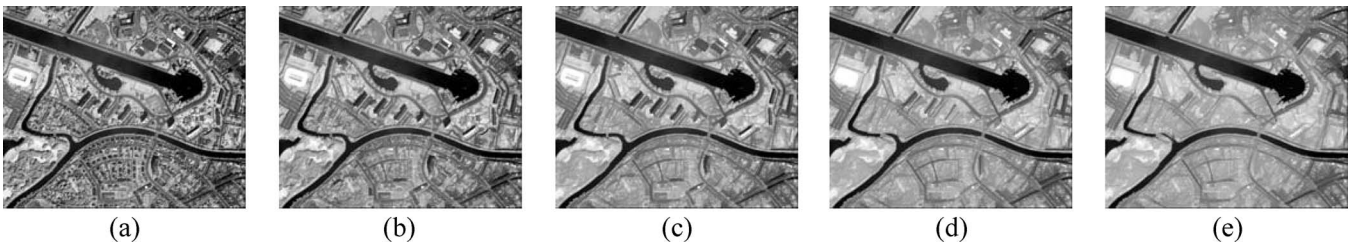

Fig. 5. Minimum of closings with linear SEs of increasing size. Objects disappear at scales corresponding to their maximum dimension. Roads remain visible at high scales, whereas buildings disappear at rather low scales. (a) Original. (b) $L = 33$. (c) $L = 65$. (d) $L = 97$. (e) $L = 129$.

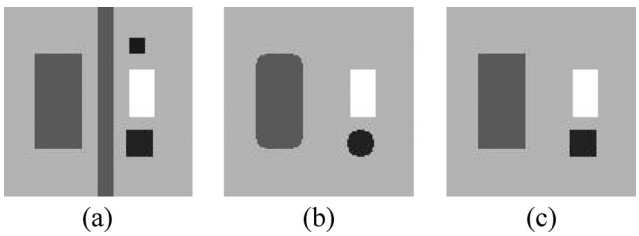

Fig. 6. (a) Image with simple structures, (b) a closing of the image, and (c) the reconstruction of the closing. The shapes of the objects are well preserved, whereas small objects still disappear.

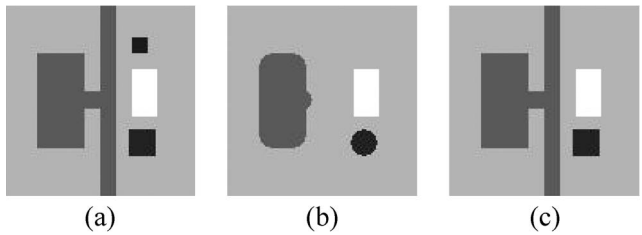

Fig. 7. (a) Image with simple but connected structures, (b) a closing of the image, and (c) the reconstruction of the closing. The long narrow object ($\propto$ road) is removed in the closing, but reconstructed in the closing with reconstruction, because of the connected broader object ($\propto$ parking lot).

from the original corner to the closest point of the pixel that was not removed equals $(\sqrt{2}-1)\cdot R$.

B. Linear SE

Aside from the disk-shaped SEs, we can also use linear SEs [18]. A line has a certain orientation θ and length L, i.e., the Euclidean distance between the two endpoints of the line (rounded off). Fig. 2 shows three closings with linear SEs of length L and different orientations using the original image in Fig. 1(a). A pixel is deleted if there exist no line of length L and orientation θ that goes through that pixel. This means that an object that is smaller than L in the orientation θ is removed. Objects which are smaller than L in all directions are removed from all these openings or closings. Therefore, the maximum of all openings with a linear SE of length L and different orientations (analogously the minimum of all closings) removes objects with a maximum dimension smaller than L. The number of orientations used to determine this maximum of openings should be chosen as high as possible, taking into account the computation time. Because of the fast algorithm [19] that exists for Bressenham lines, we can use a very dense sampling of the orientations. In our case, we use $\lfloor (1/2)\cdot L\cdot \pi \rfloor$ different orientations. Note that the maximum dimension of a rectangular object is not the length but the diagonal size. Objects with a length smaller than L, but with a diagonal size larger than L, are partly removed, beginning with the central pixels of the object sides. Fig. 3 shows a number of these transformations for different lengths L.

C. MP

By increasing the size of the SE, more and more objects are removed. We will use the term scale of an opening or closing to refer to this size. A vector containing the pixel values of pixel x in openings and closings of different scales is called the MP. The differential MP (DMP) is the vector containing the differences between subsequent values in the MP. A large value in the DMP at scale s is an indication of the presence of an object of size s. The DMP thus contains information about the size of objects. In [12], [13], and [20], the DMP has been proven useful to segment and classify remote sensing images.

In current literature, the MP is based on openings and closings with disk-shaped SEs [12], [13]. An MP based on disk-shaped SEs gives an indication of the minimum dimension of objects. Fig. 4 shows the effect of closings at different scales on an IKONOS panchromatic satellite image. As the scale increases, more and more details disappear from the image. Buildings and roads of similar width disappear at similar scales.

Fig. 8. Four scales of the disk-based MP with reconstruction. The original shapes of objects are preserved. However, a lot of the removed objects reappear because of the reconstruction. (a) Original. (b) $R = 5$. (c) $R = 10$. (d) $R = 15$. (e) $R = 20$.

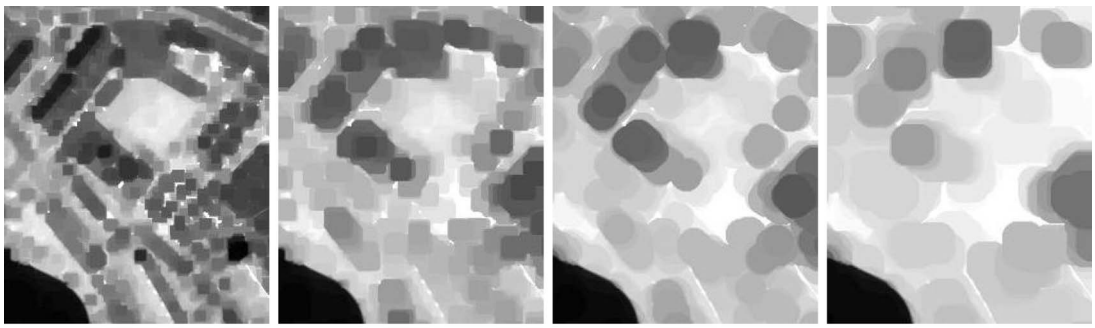

Fig. 9. Close-up of four scales of the disk-based MP (a) without and (b) with reconstruction. Some objects, which a human would consider as separate objects, are considered as a single object by the morphological reconstruction. As a result, small objects that we would expect to have disappeared are still present in all scale of the closings with reconstruction. We pointed out some typical examples with white arrows.

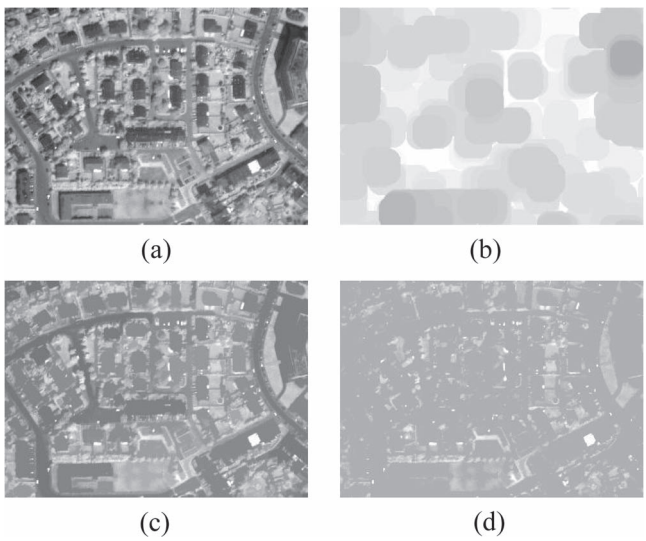

Fig. 10. Extract of the IKONOS image. Applying reconstruction (c) to the full image or (d) only to this extract results in two completely different images. Consequently, an MP with reconstruction becomes very dependent on the presence or absence of certain large objects. (a) Extract of IKONOS image. (b) Closing disk $R = 20$. (c) Reconstruction in full image. (d) Reconstruction in extract.

We also notice the blobby effect caused by the deformation of objects.

In this paper, we propose the use of an MP based on linear SEs in conjunction with the disk-based MP. Fig. 5 shows four scales (minimum of closings) of the directional MP. Where in the disk-based MP, buildings and roads disappear at more or less the same scale, here, buildings clearly disappear at much lower scales than roads. Together with the disk-based MP, the line-based MP gives a good indication of linear and nonlinear objects.

III. Reconstruction

A. Reconstruction—Over-Reconstruction

Aside from deleting objects smaller than the SE, openings and closings also deform the objects. To preserve the shapes of objects, one often uses reconstruction [21]. This process reconstructs the whole object if at least one pixel of the object survives the opening or closing. Two pixels are considered to belong to the same object if in the original image (or *mask*) they are connected. The image on which the reconstruction is performed is called the *marker*. While the use of reconstruction

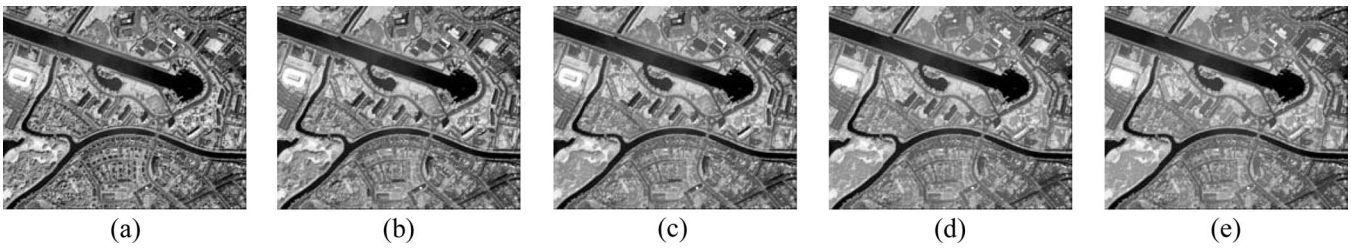

Fig. 11. Minimum of closings with linear SEs of increasing size and with reconstruction. A lot of the buildings that disappeared in the MP without reconstruction remain present in the MP with reconstruction. (a) Original. (b) $L = 33$. (c) $L = 65$. (d) $L = 97$. (e) $L = 129$.

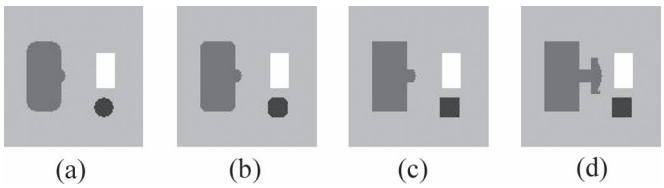

Fig. 12. Partial reconstruction of a closing of an image with connected objects. (a) and (b) When little reconstruction is applied, the corners are smoothed. (c) With more reconstruction, all corners are reconstructed. (d) When even more reconstruction is applied, connected objects start to influence each other. (a) $n = 0$. (b) $n = 2$. (c) $n = 4$. (d) $n = 16$.

has become standard, we will show that it can lead to a reduced classification performance. When dealing with an image where objects have simple shapes, the benefit of the reconstruction is minimal. For example, when an object has a constant width (e.g., a rectangle), the whole object will disappear at the same scale (except the corners, which will disappear at lower scales). In a more complex shaped object with narrowings, some parts of the object disappear at higher scales than others. In that case, reconstruction will make sure that the full object behaves as one. Typical remote sensing scenes contain mainly simple shaped objects. However, these objects are arranged in a complex manner: roads are connected to a lot of other objects, like parking lots and buildings; shadows often connect nearby dark objects, etc. These individual but connected objects are often seen as a single object by the reconstruction process, which consequently leads to a reduced classification performance.

Fig. 6 shows a closing with reconstruction on a simple image. The shapes of the objects are well preserved, whereas small objects still disappear. Fig. 7 shows a similar closing with reconstruction. In this case, however, two objects are connected through a narrow line. As a result, from a morphological point of view, the two objects are now considered as a single object. This is a typical example of what happens with roads and parking lots or roofs in remote sensing images. While the long narrow object (road) is removed in the closing, it is reconstructed afterward. This means that, in an MP, the road pixels will not be characterized by the width of the road but by the width of the largest connected object (possibly a parking lot or big roof). Clearly, this will lead to poor classification performance.

B. MP With Reconstruction

Fig. 8 shows four scales of the disk-based MP. The blobby effect in Fig. 4 is no longer visible. However, objects that have clearly been deleted in Fig. 4 remain visible on all scales in Fig. 8. The gray-scale values of small dark objects have slightly changed, but the objects did not truly disappear. This is even better illustrated in a close-up of the study area (Fig. 9). In the image, we point out two objects we would expect to disappear at a low scale but which are still present at the highest scales. Apparently, the intuitive definition of an object used by a human does not correspond with the definition of objects in mathematical morphology. As a result, the disk-based MP with reconstruction does not provide a realistic description of the minimum dimension of "objects as perceived by humans."

Fig. 10 shows an enlargement of a part of the image. Here, as well, we see that objects that have clearly disappeared reappear after the reconstruction. To further illustrate the problem, we also applied reconstruction on only this small part of the image instead of the full image. In this case, some larger objects are no longer present in the image and cannot influence the reconstruction process. When reconstruction is applied to the full image, most of the structures in the image are still present. When reconstruction is applied to only this extract, much more structures are eliminated. Consequently, an MP with reconstruction becomes very sensitive to the presence or absence of certain large objects.

Fig. 11 shows four scales of a line-based MP with reconstruction. Here, as well, we notice the same phenomena. A lot of the buildings that disappeared in the MP without reconstruction remain present in the MP with reconstruction. Also striking are the small differences between scales of the directional MP and the small difference between the directional and the disk-based MP. Apparently, the large dark objects that survive all disk- and line-based closings reconstruct almost all objects in the image.

IV. Partial Reconstruction

An MP with reconstruction clearly leads to some undesirable effects. However, without reconstruction, borders are degraded and shapes are deformed. In the ideal case, the borders would be reconstructed, whereas individual objects are still considered separate. This is not possible since it would have to automatically separate the different objects perfectly in the first place. As shown in the previous section, far away objects can influence the result of the reconstruction for a certain pixel. An improvement can be made by limiting the area of influence.

A. Definition and Implementation

To overcome the problem of over-reconstruction, we use what we call partial reconstruction. In the reconstruction

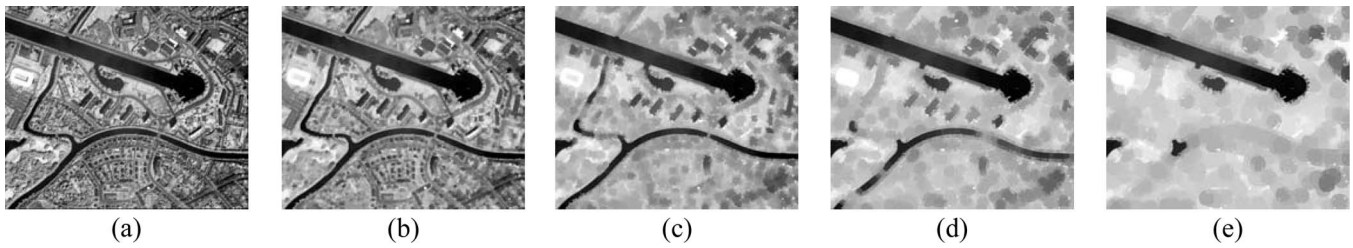

Fig. 13. Four scales of the disk-based MP with partial reconstruction. Objects do not reappear, whereas their shapes are better preserved. (a) Original. (b) $R = 5$. (c) $R = 10$. (d) $R = 15$. (e) $R = 20$.

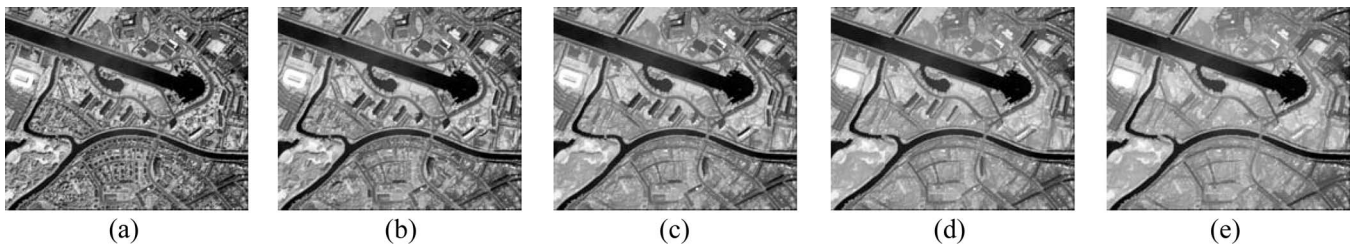

Fig. 14. Four scales of the line-based MP with partial reconstruction. Objects do not reappear, whereas their shapes are better preserved. (a) Original. (b) $L = 33$. (c) $L = 65$. (d) $L = 97$. (e) $L = 129$.

process, a pixel is reconstructed if it is connected to another pixel that was not deleted after the opening or closing. With partial reconstruction, we add a second condition. Now, a pixel is only reconstructed if it is connected to a pixel that was not erased, and this second pixel lies within a certain geodesic distance d from the pixel. The geodesic distance between two pixels is the length of the shortest path between the two pixels that lies completely within the object. If we would use the Euclidean distance instead of the geodesic distance, a large object could influence a large part of a smaller object if both objects lie close to each other, even if the connection between them is very narrow. By using the geodesic distance, only a small area of the smaller object in the neighborhood of the connection will be influenced.

The partial reconstruction as described in the previous paragraph is actually exactly the same as a geodesic dilation [17] of size d. The easiest and fastest way to implement this is by doing d successive elementary geodesic dilations. This is a dilation with an elementary SE followed by an intersection with the mask. In gray-scale morphology, the intersection of two images is the minimum of the two gray-scale values for each pixel. An elementary SE is an approximation of a disk with radius 1. In practice, this is the four-neighborhood or eight-neighborhood of a pixel. However, because these approximations are nonisotropic, the resulting geodesic dilation of size d is nonisotropic as well. Indeed, when using a four-neighborhood, the geodesic distance between two pixels would be limited to d in horizontal and vertical directions, but to $\sqrt{2}/2 \cdot d(< d)$ in the diagonal direction. Similarly, when using an eight-neighborhood, the diagonal distance would be limited to $\sqrt{2} \cdot d(> d)$. To give the partial reconstruction a more isotropic behavior, we implement the geodesic dilation with an eight-neighborhood SE, but also limit the Euclidean distance to d. This can easily be achieved by dilating the opening with a disk-shaped SE with radius d followed by the intersection with the original image. This result can then be used in the geodesic dilation as the mask instead of the original image.

B. Amount of Reconstruction

Fig. 12 shows a closing and a number of partial reconstructions with different values of d. For low values of d, corners of objects are not completely reconstructed. As d increases, more and more of the corner is reconstructed until it is completely reconstructed. When d is further increased, the connected objects start to influence each other. Because the distance between a corner and the closest not deleted pixel equals $(\sqrt{2}-1) \cdot R$ (see Section II-A), partial reconstruction with $d > (\sqrt{2}-1) \cdot R$ completely reconstructs the corners of rectangular objects. However, objects in realistic remote sensing images are not perfect rectangles. Therefore, we use partial reconstruction with $d = 2 \cdot (\sqrt{2}-1) \cdot R$.

For the MP based on linear SEs, it is more difficult to decide on a good value for the amount of reconstruction. The minimal amount necessary to completely reconstruct a rectangular object depends on the linearity of the object and is maximal for a square object. However, choosing this amount would be too high for most objects in the image. With linear SEs, rectangular objects are only deformed when the SE is larger than the length and smaller than the diagonal. Because, for most objects, the length and diagonal are of the same order of magnitude, this deformation is not a big issue. Together with information about the width of the object, pixels on linear objects are still very well distinguishable from pixels on square objects. Therefore, we do not need to do a lot of reconstruction. With linear SEs, the main goal of the reconstruction would be to reduce the influence of small obstacles (like cars) which introduce irregularities in the shape of other objects and to take care of other deviations from the rectangular shape (e.g., curved roads). We have found that a value of $d = 0.05 \cdot L$ works good. As not all of these

(a) groundtruth (b) spectral classification (c) spectral + disk and line based MP

Fig. 15. Study Area I: (a) The groundtruth, (b) classification result with only spectral information, and (c) with spectral information and disk- and line-based MPs, both with partial reconstruction. With only spectral information, there is a lot of confusion between the very dark classes water and shadow and between the man-made classes (dark roof, road, and other man-made objects). Including the two MPs improves the result substantially. Most of the road network and buildings are well classified.

effects are linearly dependent on L, it would be interesting to also investigate nonlinear functions of L.

C. MP With Partial Reconstruction

Fig. 13 shows a number of scales from the disk-based MP with partial reconstruction. While in the MP with reconstruction a lot of small objects remain present, this is not the case with partial reconstruction. Compared to the MP without reconstruction on the other hand, the shapes of objects are better preserved with partial reconstruction. Fig. 14 shows a number of scales from the line-based MP with partial reconstruction. Here, as well, we see a better preservation of shapes while short structures are removed.

V. Classification Experiments

To test and compare the different methods, we conducted a number of classification experiments. For these experiments, we used two different study areas. Both study areas lie in the neighborhood of Ghent (Belgium). For the first study area, we use an IKONOS satellite image, whereas for the second study area, a QuickBird image is used. The classification experiments are done with a multilayer perceptron (MLP), which is a kind of neural network. For each classification experiment, we tested eight different architectures with varying number of hidden nodes (25, 30, ..., 60). For each architecture, the MLP was trained five times with different initial weights. Only the results with best accuracies are reported. The results of the classifications will be discussed in the following sections.

A. Study Area I: Watersportbaan

The first study area is located in the city of Ghent (Belgium) and covers approximately 1.2 km by 1 km. An IKONOS image acquired on August 5, 2003 is used as well as an extensive groundtruth with 44 564 training samples and 486 377 evaluation samples. Fig. 15(a) shows this groundtruth.

The first column of Table I shows the producer's accuracies of the classification when only using spectral information (panchromatic image and four multispectral bands: blue, green, red, and near-infrared) and the normalized difference vegetation index (NDVI), which is a derived feature that helps to differentiate between vegetation and nonvegetation. Fig. 15(b) shows the classified image. We notice a large confusion between the classes water and shadow (both very dark) and between the man-made classes (road, dark roof, and other man-made objects). We will try to improve this result by including the MPs as extra bands in the classification.

The first MP we include is the one based on disk-shaped SEs. We use four different scales: $R = 5, 10, 15$, and 20 for both the openings and the closings. This makes a total of eight extra bands. Because an IKONOS image has a resolution of 1 m, with these four scales, it is possible to differentiate between objects of 10-, 20-, 30-, and 40-m widths. This is more or less the range of object sizes present in the image, and it allows one to differentiate between roads ($\approx$10 m) and larger buildings and open spaces. We compared the MP with reconstruction, without reconstruction, and with partial reconstruction. The resulting accuracies are shown in Table I. Compared to the situation with only spectral bands, there is a 4%–6% improvement in all three cases. For the MP without reconstruction, the main improvement lies in the different man-made classes. For example, the producer accuracy of the dark roof class increases by almost 25%. Also, the confusion between water and shadow decreases. For the MP with reconstruction, the overall accuracy is a little bit lower. In this case, however, the water and shadow classes benefit most. This is quite logical because the water in the image consists of only very few objects. Consequently, with the reconstruction, the MP of the water pixels will be very typical. The accuracies of the man-made classes, on the other hand, are much lower. The partial reconstruction is a compromise between reconstruction and no reconstruction. This also shows in the accuracies, which are comparable with the case of no reconstruction for man-made objects and a little bit worse for the shadow and water classes compared to the reconstruction method.

In this paper, we also introduced the line-based MP. The classification results based on spectral information and the line-based MPs for the three different reconstruction scenarios are

TABLE I
STUDY AREA I: PRODUCER'S ACCURACIES IN PERCENT OF A CLASSIFICATION WITH THE PANCHROMATIC BAND, FOUR MULTISPECTRAL BANDS, AND AN NDVI FEATURE BAND (COLUMN 1), COMPARED TO CLASSIFICATIONS WITH THESE SIX SPECTRAL-BASED BANDS AND EIGHT ADDITIONAL DISK-BASED MP BANDS WITHOUT RECONSTRUCTION (COLUMN 2), WITH RECONSTRUCTION (COLUMN 3), AND WITH PARTIAL RECONSTRUCTION (COLUMN 4)

class	spectral only	no reconstr.	reconstr.	partial reconstr.
water	92.62	94.00	**97.73**	95.02
grass	71.41	69.03	72.32	**72.50**
trees	83.42	**88.69**	88.19	86.53
dark roof	37.80	61.95	46.52	**62.49**
red roof	52.57	**73.92**	52.85	62.51
white roof	**86.43**	84.06	80.09	80.09
road	55.48	**72.55**	69.97	71.41
other man-made	**54.05**	49.04	45.44	53.21
shadow	41.03	50.77	**61.13**	57.95
Overall Accuracy	72.15	77.13	76.57	**78.09**

TABLE II
STUDY AREA I: PRODUCER'S ACCURACIES IN PERCENT FOR CLASSIFICATIONS WITH SIX SPECTRAL-BASED BANDS AND EIGHT LINE-BASED MP BANDS. COMPARISON OF THE PERFORMANCE WHEN USING RECONSTRUCTION, NO RECONSTRUCTION, AND PARTIAL RECONSTRUCTION

class	no reconstruction	reconstruction	partial reconstruction
water	98.36	98.37	**98.47**
grass	72.36	70.64	**72.78**
trees	84.12	85.83	**86.00**
dark roof	**55.17**	46.67	53.83
red roof	58.31	52.44	**58.44**
white roof	**84.01**	81.78	83.43
road	67.89	68.53	**68.75**
other man-made	**53.23**	47.68	53.22
shadow	61.01	**63.30**	61.26
Overall Accuracy	77.54	76.23	**77.98**

shown in Table II. In this case, we use SE sizes of 33, 65, 97, and 129 for both openings and closings. This range of scales allows one to differentiate between very short objects (isolated houses, < 33 m), larger buildings and open spaces ($\approx$100 m), and long roads (> 129 m). Again, we see a clear improvement over the case that uses only spectral information. The results for the shadow and water classes are quite similar for the three scenarios and somewhat better than with the disk-based MP with reconstruction. All the water pixels in the image belong to very long objects and therefore are well separable from shadow. The results for the man-made classes are a bit worse than with the disk-based MP. The directional MP allows one to differentiate between small buildings and roads. However, larger buildings and building blocks are easily confused with short and curved roads. The results for the man-made classes for the MP with reconstruction are again substantially worse than without reconstruction. The partial reconstruction seems again a good compromise.

Finally, we also include both the disk-based and the line-based MP in the classification process. In this case, we have six spectral bands, eight disk-based MP bands, and eight

TABLE III
STUDY AREA I: PRODUCER'S ACCURACIES IN PERCENT FOR CLASSIFICATIONS WITH SIX SPECTRAL-BASED BANDS, EIGHT DISK-BASED MP BANDS, AND EIGHT LINE-BASED MP BANDS

class	no reconstruction	reconstruction	partial reconstruction
water	98.12	98.56	**98.75**
grass	72.52	74.35	**75.40**
trees	**87.40**	85.77	85.64
dark roof	68.59	50.61	**68.60**
red roof	69.11	58.52	**72.37**
white roof	83.62	81.83	82.51
road	72.86	71.90	**74.47**
other man-made	**58.99**	45.78	58.35
shadow	**65.32**	63.16	63.41
Overall Accuracy	80.92	77.28	**81.10**

(a) spectral only (b) disk based MP (c) directional MP (d) disk based + directional MP

Fig. 16. Details of Study Area I: Comparison of classifications (a) with only spectral information, (b) with spectral information and a disk-based MP or (c) a directional MP, or (d) with both. With the disk-based MP, confusion remains between small roofs and roads. With the directional MP, larger roofs and curved roads are confused. Combining both disk-based and directional MPs allows one to differentiate between almost all roads and all roofs.

directional MP bands. Table III contains the results of the classification. There is a substantial improvement of the overall accuracy over the classifications with only the disk-based or line-based MP. However, when using reconstruction, the accuracy improves only very little and is comparatively much lesser than without reconstruction. This confirms our hypothesis that the reconstruction process is very much influenced by some large objects in the image. Therefore, the line-based MP and disk-based MP with reconstruction contain much the same information. Fig. 15(c) shows the classification result with spectral information and the two MPs with partial reconstruction. Most of the road network and buildings are well classified.

Fig. 16 shows the comparison between the classifications with disk-based MP, directional MP, or both on some details of the study area. With only spectral information, there is a lot of confusion between water and shadow and between the different man-made classes. When adding the disk-based MP, we see a clear improvement. Most of the water and shadow

(a) panchromatic QuickBird image (b) groundtruth (c) spectral classification (d) spectral + disk and line based MP

Fig. 17. Study Area II: (a) The QuickBird panchromatic image, (b) the groundtruth, (c) a classification result with only spectral information, and (d) a classification result with spectral information, a disk-based MP, and a line-based MP, both with partial reconstruction. (a) Panchromatic QuickBird image. (b) Groundtruth. (c) Spectral classification. (d) Spectral + disk- and line-based MPs.

TABLE IV
STUDY AREA II: PRODUCER'S ACCURACIES IN PERCENT OF A CLASSIFICATION WITH THE PANCHROMATIC BAND, FOUR MULTISPECTRAL BANDS AND AN NDVI FEATURE BAND (COLUMN 1), COMPARED TO CLASSIFICATIONS WITH THESE SIX SPECTRAL-BASED BANDS, EIGHT DISK-BASED MP BANDS, AND EIGHT DIRECTIONAL MP BANDS WITHOUT RECONSTRUCTION (COLUMN 2), WITH RECONSTRUCTION (COLUMN 3), AND WITH PARTIAL RECONSTRUCTION (COLUMN 4)

class	spectral only	no reconstr.	reconstr.	partial reconstr.
bare soil	**95.48**	94.76	93.90	94.25
grass	89.05	84.85	83.09	**89.61**
trees	80.40	**91.19**	89.34	88.69
road	53.74	64.41	56.81	72.14
roof	75.46	**94.10**	79.75	93.07
Overall Accuracy	79.87	88.02	82.29	**88.95**

are now well classified, and the road and building classes are also better distinguished. The small buildings in the top row are, however, still easily confused with the road class. When replacing the disk-based MP with the directional MP, this last confusion decreases. On the other hand, since the image contains a lot of larger buildings, the roads are now confused with those buildings. In particular, a lot of the curved roads are misclassified, as they will seem to have a smaller length than straight roads. When using both disk-based and directional MPs, we are able to distinguish roads from both small and large buildings.

B. Study Area II: Sint-Denijs-Westrem

The second study area is located in Sint-Denijs-Westrem near Ghent (Belgium). The classification is based on a QuickBird image. We used 37 911 training samples and 807 100 evaluation samples. Fig. 17(a) and (b) shows the panchromatic image and the groundtruth, respectively.

The first column of Table IV shows the classification accuracies when only using spectral information, whereas the classified image is in Fig. 17(c). Columns 2–4 of Table IV show the accuracies when including both disk-based and line-based MPs. Although the resolution of a QuickBird image is a bit higher (70 cm) than that of an IKONOS image, we use the same scales as for Study Area I. The objects in Study Area II are generally smaller than those in Study Area I, which justifies this choice. For the case without reconstruction and the case with partial reconstruction, we see a substantial improvement of the classification result, particularly for the classes road and roof. However, with reconstruction, the accuracy is much lower. The partial reconstruction performs marginally better than no reconstruction. Fig. 17(d) shows the classification result with spectral information and both MPs with partial reconstruction.

VI. CONCLUSION

Past research has showed promising results for including geometrical information in the classification process using mathematical morphology. Previous methods use an MP based on disk-shaped SEs. In this paper, we introduced an MP based on linear shaped SEs. Our results show substantial improvement in classification when combined with the disk-based MP. With only one MP, we have six spectral features and eight spatial features. With two MPs, as proposed here, we have 16 spatial features. While we see a clear improvement of the classification, this increase in dimensionality might have a negative influence on the classification algorithm, particularly because the amount of information in the 16 spatial feature bands is rather limited and the different scales are highly correlated. Possibly, even better results could be achieved when using a feature extraction algorithm [13], [22] prior to classification. Because the different types of information lead to better results on some classes and worse on others, hierarchical classification [6] or decision fusion [23], [24] could also further improve the results.

In this paper, we also addressed the problem of over-reconstruction. Because of its ability to preserve the shape of objects, it has become standard practice to use morphological reconstruction. However, we show that this leads to over-reconstruction with possibly decreased classification performances as a result. A new method called "partial reconstruction" is proposed, which is able to overcome the problem of over-reconstruction and to still preserve the shapes of objects as much as possible. Classification experiments have shown a large increase in classification performance when not using reconstruction. With partial reconstruction, the classification is further improved.

REFERENCES

[1] Q. Zhang and I. Couloigner, "Automated road network extraction from high resolution multi-spectral imagery," in *Proc. ASPRS Annu. Conf.*, Reno, NV, May 1–5, 2006.

[2] Z. Liu, J. Wang, and W. Liu, "Building extraction from high resolution imagery based on multi-scale object oriented classification and probabilistic hough transform," in *Proc. IGARSS*, Seoul, South Korea, 2005, pp. 2250–2253.

[3] A. M. Marangoz, M. Oruc, and G. Buyuksalih, "Object-oriented image analysis and semantic network for extracting the roads and buildings from ikonos pan-sharpened images," in *Proc. ISRPS Annu. Conf.*, Istanbul, Turkey, Jul. 19–23, 2004.

[4] P. Hofmann, "Detecting urban features from Ikonos data using an object-oriented approach," in *Proc. RSPS*, 2001, pp. 79–91.

[5] A. K. Shackelford and C. H. Davis, "A combined fuzzy pixel-based and object-based approach for classification of high-resolution multispectral data over urban areas," *IEEE Trans. Geosci. Remote Sens.*, vol. 41, no. 10, pp. 2354–2363, Oct. 2003.

[6] A. Shackelford and C. Davis, "A hierarchical fuzzy classification approach for high-resolution multispectral data over urban areas," *IEEE Trans. Geosci. Remote Sens.*, vol. 41, no. 9, pp. 1920–1932, Sep. 2003.

[7] L. Zhang, X. Huang, B. Huang, and P. Li, "A pixel shape index coupled with spectral information for classification of high spatial resolution remotely sensed imagery," *IEEE Trans. Geosci. Remote Sens.*, vol. 44, no. 10, pp. 2950–2961, Oct. 2006.

[8] X. Huang, L. Zhang, and P. Li, "Classification and extraction of spatial features in urban areas using high-resolution multispectral imagery," *IEEE Geosci. Remote Sens. Lett.*, vol. 4, no. 2, pp. 260–264, Apr. 2007.

[9] J. Serra, *Image Analysis and Mathematical Morphology*. London, U.K.: Academic, 1982.

[10] P. Soille and M. Pesaresi, "Advances in mathematical morphology applied to geoscience and remote sensing," *IEEE Trans. Geosci. Remote Sens.*, vol. 40, no. 9, pp. 2042–2055, Sep. 2002.

[11] P. Soille, *Morphological Image Analysis: Principles and Applications*, 2nd ed. Berlin, Germany: Springer-Verlag, 2003.

[12] J. Chanussot, J. A. Benediktsson, and M. Fauvel, "Classification of remote sensing images from urban areas using a fuzzy possibilistic model," *IEEE Geosci. Remote Sens. Lett.*, vol. 3, no. 1, pp. 40–44, Jan. 2006.

[13] J. A. Benediktsson, M. Pesaresi, and K. Arnason, "Classification and feature extraction for remote sensing images from urban areas based on morphological transformations," *IEEE Trans. Geosci. Remote Sens.*, vol. 41, no. 9, pp. 1940–1949, Sep. 2003.

[14] J. Benediktsson, J. Palmason, and J. R. Sveinsson, "Classification of hyperspectral data from urban areas based on extended morphological profiles," *IEEE Trans. Geosci. Remote Sens.*, vol. 43, no. 3, pp. 480–491, Mar. 2005.

[15] J. Chanussot, G. Mauris, and P. Lambert, "Fuzzy fusion techniques for linear features detection in multitemporal SAR images," *IEEE Trans. Geosci. Remote Sens.*, vol. 37, no. 3, pp. 1292–1305, May 1999.

[16] S. Sigurjonsson, J. Benediktsson, J. Sveinsson, G. Lisini, P. Gamba, and J. Chanussot, "Street tracking based on sar data from urban areas," in *Proc. IGARSS*, 2005, pp. 1273–1276.

[17] C. Lantuejoul and F. Maisonneuve, "Geodesic methods in quantitative image analysis," *Pattern Recognit.*, vol. 17, no. 2, pp. 177–187, 1984.

[18] P. Soille and H. Talbot, "Directional morphological filtering," *IEEE Trans. Pattern Anal. Mach. Intell.*, vol. 23, no. 11, pp. 1313–1329, Nov. 2001.

[19] P. Soille, E. J. Breen, and R. Jones, "Recursive implementation of erosions and dilations along discrete lines at arbitrary angles," *IEEE Trans. Pattern Anal. Mach. Intell.*, vol. 18, no. 5, pp. 562–567, May 1996.

[20] M. Pesaresi and J. A. Benediktsson, "A new approach for the morphological segmentation of high-resolution satellite imagery," *IEEE Trans. Geosci. Remote Sens.*, vol. 39, no. 2, pp. 309–320, Feb. 2001.

[21] J. Crespo, J. Serra, and R. Shafer, "Theoretical aspects of morphological filters by reconstruction," *Signal Process.*, vol. 47, no. 2, pp. 201–225, Nov. 1995.

[22] J. C.-W. Chan, R. Bellens, F. Canters, and S. Gautama, "An assessment of geometric activity features for classification of urban man-made objects using very-high-resolution imagery," *Photogramm. Eng. Remote Sens.*, 2008, to be published.

[23] M. Fauvel, J. Chanussot, and J. Benediktsson, "Decision fusion for the classification of urban remote sensing images," *IEEE Trans. Geosci. Remote Sens.*, vol. 44, no. 10, pp. 2828–2838, Oct. 2006.

[24] B. Waske and J. Benediktsson, "Fusion of support vector machines for classification of multisensor data," *IEEE Trans. Geosci. Remote Sens.*, vol. 45, no. 12, pp. 3858–3866, Dec. 2007.

Rik Bellens (S'07) received the diploma in computer science engineering from Ghent University, Ghent, Belgium, in 2004, where he is currently working toward the Ph.D. degree in the Department of Telecommunications and Information Processing.

From 2004 to 2005, he worked on different remote sensing projects. Since 2006, he has had a scholarship of the "Institute for the Promotion of Innovation through Science and Technology in Flanders" (IWT-Vlaanderen). His main research interests include pattern recognition, remote sensing, and image processing.

Sidharta Gautama (M'05) received the M.Sc. and Ph.D. degrees in electrical engineering from Ghent University, Ghent, Belgium, in 1994 and 2002, respectively.

From 1994 to 2005, he was with the Department of Telecommunication and Information Processing, Ghent University, as an Assistant Professor in the field of computer vision and artificial intelligence. Since 2006, he has been working in technology transfer and development with Ghent University in the field of information management (iKNOW research cluster). He manages the UGent intellectual property for the Incubator for Geoinformation and is a Chairman of the Institute of Spatial Information of Ghent University. His main research interests include pattern recognition, graph-based object models, performance characterization/prediction, and scene understanding.

Leyden Martinez-Fonte (S'03–M'04) received the B.S. and M.Sc. degrees in electrical engineering and applied informatics from the Higher Polytechnic Institute José Antonio Echeverría, Havana, Cuba, in 1994 and 1997, respectively. Since 2003, she has been working toward the Ph.D. degree in applied sciences at Ghent University, Ghent, Belgium.

From 1994 to 2003, she was with the Departments of Telecommunications and Automation, Higher Polytechnic Institute José Antonio Echeverría, where she became an Assistant Professor. From 1999 to 2002, she was a Project Manager with Copextel S.A. for the development of software products. Her research interests include software engineering and image processing.

Wilfried Philips (S'90–M'93) was born in Aalst, Belgium, on October 19, 1966. He received the Diploma degree in electrical engineering and the Ph.D. degree in applied sciences from Ghent University, Ghent, Belgium, in 1989 and 1993, respectively.

From October 1989 to October 1997, he was with the Department of Electronics and Information Systems, Ghent University, for the Flemish Fund for Scientific Research (FWO-Vlaanderen), first as a Research Assistant and later as a Postdoctoral Research Fellow. Since November 1997, he has been with the Department of Telecommunications and Information Processing, Ghent University, where he is currently a full-time Professor and is heading the research group "Image Processing and Interpretation," which has recently become part of the virtual Flemish ICT research institute IBBT. Some of the recent research activities in the group include image and video restoration and analysis and the modeling of image reproduction systems. Important application areas targeted by the group include remote sensing, surveillance, and industrial inspection.

Jonathan Cheung-Wai Chan received the B.S. and M.S. degrees in geography from the Chinese University of Hong Kong, Shatin, Hong Kong, and the Ph.D. degree from the Center of Urban Planning and Environmental Management, Hong Kong University, Hong Kong, in 1999.

Between 1998 and 2001, he was a Research Scientist with the Department of Geography, University of Maryland, College Park. During that time, his main research subjects were machine learning algorithms for global land cover classification and long-term monitoring of global land cover changes. From 2001 to 2005, he was with Vrije Universiteit Brussel (VUB) and the Interuniversity Microelectronics Research Center, Belgium, working for European projects that apply remote sensing methods for landmine detection and minefield area reduction. His main research areas were multispectral analysis using multilevel acquisitions of thermal infrared images. Since October 2005, he has been with the Department of Geography, VUB, where he currently teaches introductory and advanced remote sensing courses. His main research interests include machine learning algorithms, hyperspectral analysis, superresolution image reconstruction, textural classification, change detection, and information retrieval from remote sensing images. He conducts and supervises research on these topics within the framework of several nationally funded projects.

Frank Canters received the M.Sc. degrees in geography and applied computer science, and the Ph.D. degree in sciences from Vrije Universiteit Brussel (VUB), Brussels, Belgium, in 1999.

Between 1999 and 2001, he was with the Department of Geography, VUB, as a Postdoctoral Researcher, where he is currently an Associate Professor and has been leading the Cartography and GIS Research Unit since 2002. He is also a Visiting Professor with Ghent University. His is teaching undergraduate courses in cartography, geoinformation science, and spatial analysis, and master courses in Earth observation, spatial data quality, and map projection. His main research interests include urban remote sensing, multiresolution image analysis, modeling of uncertainty in spatial data, and map projection design.